CHAPTER-6

MULTI OBJECTIVE OPTIMIZATION OF DOUBLE EFFECT SERIES AND PARALLEL FLOW WATER–LITHIUM CHLORIDE AND WATER–LITHIUM BROMIDE SYSTEMS

CHAPTER-6

MULTI OBJECTIVE OPTIMIZATION OF DOUBLE EFFECT SERIES AND PARALLEL FLOW WATER–LITHIUM CHLORIDE AND WATER–LITHIUM BROMIDE SYSTEMS

6.1 Introduction

Detail parametric analysis was done in Chapter 4 and Chapter 5 to evaluate the energetic and exergetic performance of the double effect VARS configurations with H_2O–LiCl as working solution pair. Energetic and exergetic performance comparison with H_2O–LiBr operated double effect systems was also provided separately in Chapter 4 and 5. In this research study, as described in the previous two chapters (Chapter 4 and Chapter 5), it was attempted to find out the optimal temperature difference between the HPG and LPG temperatures (T_{LPG} and T_{HPG}) in the H_2O–LiCl operated double effect series, parallel and reverse parallel configuration for four different cases (Case 1, Case 2, Case 3 and Case 4) of fixed condenser (also equal absorber) and evaporator temperatures. For the parallel and reverse parallel configurations, additionally, the optimal distribution ratio was also tried to be found out. However, in Chapter 4 and 5, it was done parametrically with lot of maneuvering in the computer simulation programs through (i) simultaneous change in T_{LPG} and $T_{HPG}$and (ii) change in T_{HPG}at fixed T_{LPG} to find out the optimal T_{LPG} and T_{HPG} for various cases. Since some difficulties were faced in finding out the optimal parameters through parametric analysis in Chapter 4 and 5, particularly the optimal operating conditions of the double effect parallel configuration, therefore, it was felt that an optimization study, using evolutionary based genetic algorithm (GA), would be more appropriate for finding the optimal operating conditions of the double effect series and parallel absorption refrigeration systems. The reverse parallel system is not considered for optimization because the range of operating conditions was found to be low for this particular configuration.

From literature review in Chapter 2 also, it was found that double effect VARS configurations were not optimized earlier to maximize their performances using evolutionary based optimization techniques. As such, optimization study using evolutionary based GA was never done earlier for double effect H_2O–LiCl and H_2O–LiBr VARS configurations. Therefore, in this research study, a GA based multi-objective

optimization is performed on the double effect series and parallel configurations in order to find out the optimum performance of the two system configurations and also to provide a comparative assessment between H_2O–LiCl and H_2O–LiBr based systems at the optimized operating conditions. Two MATLAB programs, one for the systems' simulation and the other for the GA were developed and coupled to find the optimal results. For the multi-objective optimization, the system's COP, exergy efficiency (η) and the total irreversibility $(\dot{I}_{tot})$ are taken as objective functions. In the series configuration, the HPG and LPG temperatures are the two decision variables while for the parallel configuration, additionally the distribution ratio *(D)* is also considered as a decision variable. The optimal combinations of HPG and LPG temperatures and *D* are determined for four various cases of fixed evaporator and condenser (also equal absorber) temperatures and presented in this chapter along with the optimized performance parameters (COP, exergy efficiency and total irreversibility). Since the flow schematics of the double effect series and parallel configurations were already described in Chapter 4; hence these are not repeated in this chapter.

6.2 Assumptions

The assumptions made in this optimization study are almost similar with those presented in Chapter 4 and Chapter 5. Here also, it is assumed that the refrigerant is saturated liquid and saturated vapour respectively at the condenser and evaporator outlets. The pressure in the absorber and the evaporator is considered equal. Equal operating pressure is assumed also in the condenser and the LPG. Further, it is assumed that the strong refrigerant solution at absorber exit is saturated liquid mixture at absorber pressure and temperature. Similarly, the medium and weak solutions at HPG and LPG exits are saturated liquid mixtures at their respective generator pressure and temperature. Temperature of saturated steam (HPG heat source) is considered 10°C higher than the HPG temperature. Evaporator cooling load is fixed 350 kW. Motor efficiency is 90% while the efficiencies of SHE I and SHE II are considered 75%. Water temperatures at inlet and outlet of the condenser and absorber are considered as 25°C and 30°C respectively. Evaporator inlet and outlet water temperatures are taken as 15°C and 10°C respectively. Condenser and absorber temperatures (T_C and T_A) are set equal. Some constraints are imposed during double effect VARS optimization. The maximum solution concentration at LPG exit for the H_2O–LiCl system is not allowed to exceed

50% while the same for the H_2O–LiBr system is restricted within 65%. Negative irreversibility in any system component is avoided during the optimization process. Further, the weak solution concentration at LPG exit, in no case, is allowed to be less than the strong solution concentration at absorber exit.

6.3 System modelling

The model s used for simulating the double effect series and parallel configurations are the same with those presented in Chapter 4 and Chapter 5. Just to repeat in short, thermodynamic properties of H_2O–LiCl solution are calculated using the correlations of Patek and Klomfar [1]. The medium solution concentration at the HPG exit (X_8) is calculated in an iterative manner such that it satisfies the energy balance in the LPG [2, 3]. The strong and weak solution concentrations (X_4 and X_{15}) at the absorber and LPG outlets are calculated iteratively using property equations taken from Ref. [1]. From known medium solution concentration at HPG exit (X_8) and HPG temperature, next the HPG pressure is determined using correlations given in Ref. [1] through an iterative procedure. The same procedure is followed for H_2O–LiBr mixture while its properties are calculated from correlations given in Ref. [4]. Thermodynamic properties of liquid water and water vapour (steam) are computed using equations taken from International Associations for the Properties of Water and Steam (IAPWS) formulation 1997 [5]. The following general mass and energy balance equations of steady flow processes are applied in modeling the VARS components.

Mass conservation:

$$\sum \dot{m}_{in} = \sum \dot{m}_{out} \tag{6.1}$$

$$\sum \dot{m}_{in} X_{in} = \sum \dot{m}_{out} X_{out} \tag{6.2}$$

Energy Conservation:

$$\sum \dot{Q} - \sum \dot{W} = \sum (\dot{m}h)_{in} - \sum (\dot{m}h)_{out} \tag{6.3}$$

The D involved with the double effect parallel (Refer Chapter 4, Fig. 4.2a) configuration is defined as follows.

$$D = \frac{\dot{m}_{6a}}{\dot{m}_4} \tag{6.4}$$

From mass balance, the solution concentration at absorber inlet of the parallel configuration, in terms of D, X_8 and X_{15}, can be expressed as follows

$$X_{17} = \frac{1}{\left[\frac{D}{X_8} - \frac{1-D}{X_{15}}\right]} \tag{6.5}$$

Effectiveness method is used to calculate solution temperatures at the outlets of SHE I and SHE II. The mass flow rate of refrigerant $(\dot{m}_r)$ is determined from known evaporator cooling load $(\dot{Q}_E)$as follows.

$$\dot{m}_r = \frac{\dot{Q}_E}{h_3 - h_2} \tag{6.6}$$

The amount of steam required in the HPG of the double effect VARS is calculated using the following equation.

$$\dot{m}_{s,HPG} = \frac{\dot{Q}_{HPG}}{h_{18} - h_{19}} \tag{6.7}$$

where $\dot{Q}_{HPG}$ is the HPG heat load.

COP of the double effect system is: $COP = \frac{\dot{Q}_E}{\dot{Q}_{HPG} + \dot{W}_{SP}}$, (6.8)

$\dot{W}_{SP}$ in Eq. (6.8) is the SP pumping power.

The following general exergy balance equation is used to calculate exergy destruction (or irreversibility) in various components of the double effect VARSs.

$$\sum \dot{E}x_{in} - \sum \dot{E}x_{out} - \dot{Q}\left(1 - \frac{T_0}{T}\right) - \dot{W} - \dot{E}x_d = 0 \tag{6.9}$$

The exergy efficiency is estimated using the following equation.

$$\eta = \frac{\dot{E}x_{w,E_{out}} - \dot{E}x_{w,E_{in}}}{\dot{E}x_{s,HPG_{in}} - \dot{E}x_{s,HPG_{out}} + \sum \dot{W}_{SP}} \tag{6.10}$$

where $\dot{E}x$ is the total exergy, the product of mass flow rate and specific exergy. The total system irreversibility $\left(\dot{I}_{tot}\right)$is determined by summing up the exergy destruction i.e. $\dot{E}x_d$ (or irreversibility $\dot{I}$) in all the VARS components.

6.4 Genetic algorithm

GA is one class of evolutionary algorithms that is often used to find optimal solutions of many engineering problems. It is based on techniques inspired by natural evolution. Initialization, selection, crossover and mutation: these are the four basic operations associated with GA. Details about GA are available in the articles [6, 7]. The GA operations are described briefly in the following section.

6.4.1 Initialization

The first step in GA is population initialization. GA uses a set of probable solutions called parents to search for the optimal solution. The total number of probable solutions is called population size (NP). The population is initialized through random selection of initial parameter values uniformly within the search space (entire range of possible solutions) from the defined lower and upper bounds ($Y^{(L)}$ and $Y^{(U)}$) of the parameters as follows.

$$\begin{aligned} &Y_i = Y^{(L)} + rand \in (0,1) \times \left(Y^{(U)} - Y^{(L)}\right) \\ &i = 1, 2, \ldots, \text{NP} \end{aligned} \tag{6.11}$$

where $rand \in (0,1)$ represents a uniformly distributed random variable within the range [0, 1]. The population size NP depends on the nature of the problem and typically contains several hundreds of possible solutions**.** In this Chapter, population size (NP) is taken 600 for the series configuration and 800 for the parallel configuration. The lower and upper bounds of decision variables are shown in Table 6.1**.**

Table 6.1: Range of lower and upper bounds of decision parameters

H_2O–LiCl	Range	H_2O–LiBr	Range
LPG temperature:	60 – 80°C	LPG temperature:	65 – 90°C
HPG temperature:	85 – 130°C	HPG temperature:	95 – 145°C
Distribution ratio for parallel system	0.4 – 0.8	Distribution ratio for parallel system	0.3 – 0.8

6.4.2 Selection

During the selection process, superior (fittest) individuals are selected based on their fitness. In GA, an individual is characterized by a set of variables called genes. Genes are encoded into a string to form chromosomes (solutions). A chromosome in GA is therefore a string in the form of array of bits and the value of the bits in the array is usually shown in binary form (either 0 or 1). Fitness is found with the help of a defined fitness function. The fitness function gives a fitness score to each individual and this fitness score decides the probability of an individual for its selection in the crossover operation. The fitness function is usually problem dependent and defined in such a way that only the best solutions are selected. However to maintain genetic diversity in the population and also to prevent premature convergence, a small portion of comparatively less fit solutions are also allowed to enter the population of the next generation. The number of individuals allowed to pass on their genes to the next generation may vary according to the selection operator used. In this Chapter, 50% of population (NP) is used to generate next generation individuals (offspring) of size NP. The following fitness function is used in the present multi-objective optimization problem.

$$\text{Fitness}=1-\frac{1}{N}\sum_{i=1}^{N}\left(\frac{1}{f_i\left(Y_j\right)+1}\right) \tag{6.12}$$

$$\text{where, } f_i\left(Y_j\right)=\begin{cases} abs\left\{f_i\left(Y_j\right)\right\}\ ;\ \text{if} f_i\left(Y_j\right)\ \text{is to be minimized} \\ \dfrac{1}{abs\left\{f_i\left(Y_j\right)\right\}};\ \text{if} f_i\left(Y_j\right)\ \text{is to be maximized} \end{cases}$$

and $f\left(Y_j\right)$ is the objective function as a function of Y_j, the decision parameters.

6.4.3 Cross-over

Crossover is the most important process of GA. It is performed to generate the next generation of population (offspring) from a pair of parent solutions. Many crossover techniques are available (one point, two point, uniform and half uniform and three parents etc.). The most common is the single point crossover. In single point crossover, a single crossover point is chosen randomly from within the genes as shown in Fig. 6.1 below. Offspring are produced through exchange of genes from either side up to the crossover point which are then added to the new population based on their fitness. During crossover, as shown in Fig. 6.2, the offspring (children) take one section of the chromosome from each parent. As in a natural process, every parent is not able to produce offspring so this is implemented in GA by using a parameter called cross-over probability (CP). A good choice for CP is between 60% and 70% which means, a good number of parents will bear offspring. In this Chapter, cross over probability is taken 70%.

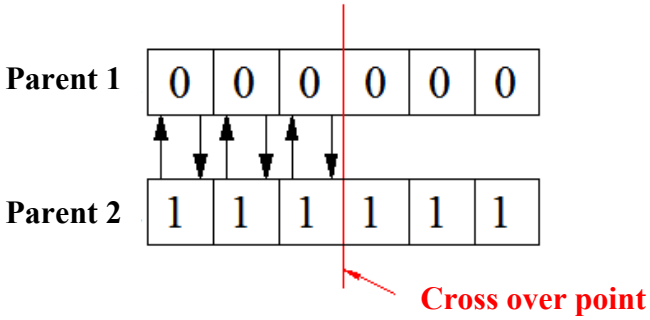

Fig. 6.1: Exchange of genes between two parent solutions

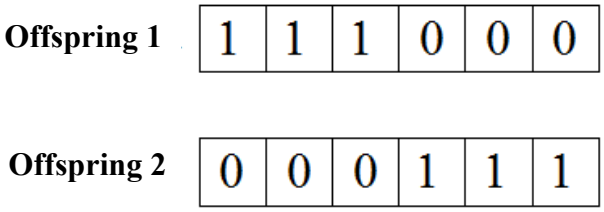

Fig. 6.2: Generation of new offspring

6.4.4 Mutation

Mutation is performed in GA to maintain genetic diversity in the solutions through flipping of some of the bits in the bit string (alteration of gene values in chromosomes). After mutation, the solutions change entirely from its previous solutions. This is shown in Fig. 6.3. It is used mainly to obtain better solutions without premature convergence. Mutation is performed in accordance with a user-defined parameter called mutation probability. Mutation probability is usually set to be low and a relatively high value of mutation probability leads to a primitive random search. In this Chapter, the mutation probability is set 0.01. After mutation, the binary chromosomes are converted back to decimal form and the fitness score of all individuals is evaluated. Commonly, the GA terminates either after certain maximum number of generations are produced or a satisfactory fitness level is reached for the population. In the present study, the maximum 200 number of generations is considered and this is also set as the terminating criteria. The termination of GA indicates that the optimum solution is reached.

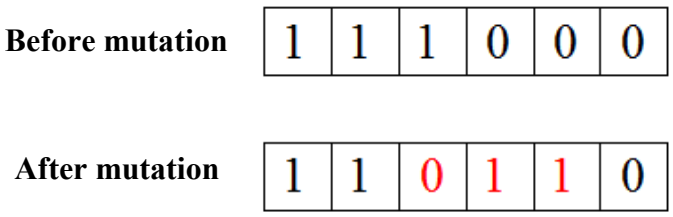

Fig. 6.3: Mutation

6.4.5 Non-dominated sorting

Next sorting of the solutions in the final population is done based on non-domination. Each solution is compared with the rest of the solutions in the population to find if it is dominated. Suppose, if a solution 'X' dominates any solution 'Y' in the population, then the solution 'Y' is rejected temporarily. Otherwise, if the solution 'X' is dominated by any individual in the population, the solution 'X' is rejected. If the solution 'X' is not dominated by any other individual, then it becomes the best non dominated solution and this is how the individuals of first set of best Pareto front (PF1) are selected. Therefore, depending on situations, either a single or a number of solutions may appear in PF1. These solutions in PF1 are superior to the others at least either in terms of maximum COP or in terms of maximum exergy efficiency or minimum irreversibility. Next, the solutions of PF1 are discounted temporarily and the

above procedure is repeated for the left over solutions to find the remaining non-dominated PFs (PF2, PF3 etc.). The step-by-step GA procedures are described below.

Step 1: An initial population of each decision parameter of size NP is selected randomly from within the defined lower and upper bounds of the parameters.

Step 2: The fitness score of each individual is evaluated and starting from the solution with the least fitness score in ascending order, 50% of the population is selected for further evaluation.

Step 3: Genes are encoded to the selected individuals to form binary chromosomes.

Step 4: Cross over is performed between a pair of parent chromosomes (solutions) to generate the next generation of population (offspring) of size NP.

Step 5: Mutation is performed to alter the gene values of the chromosomes.

Step 6: The individuals in the form of binary chromosomes are converted back to decimal form and their fitness score is evaluated.

Step 7: If the fitness scores of some of the best individuals (number of best individuals is user defined) are less than a prescribed minimum value (0.001), then it implies that the optimum solution is reached.

Step 8: If the condition in Step 7 is not satisfied, the procedures from Step 3 to Step 7 are repeated on the entire population generation after generation until the stopping criterion is satisfied. The number of times the procedures from Step 3 to Step 7 are repeated is actually the number of generations.

Step 9: Once the optimum solution is reached, the non-dominated sorting is done to find the PFs. The flow chart of the GA is shown in Fig. 6.4.

Fig. 6.4: Flow Chart of Genetic Algorithm

6.5 More about the fitness function

The fitness function (Eq. 6.12 in section 6.4.2) used in this study is a simple mathematical equation where the fitness function assumes a minimum value when it is used for a set of objective functions. Say for example in a given system, its cost is to be minimized and efficiency is to be maximized. The number of objective functions in this case is two (cost and efficiency) and considering the following three cases it may be shown that the fitness function values for Case 1, Case 2 and Case 3 are 0.777761, 0.794103 and 0.763145 respectively.

Case 1: Cost Rs. 30000.00 and efficiency 80%

Case 2: Cost Rs. 35000.00 and efficiency 70%

Case 3: Cost Rs. 40000.00 and efficiency 90%

Thus among the three cases, Case 3 presents a comparatively better solution compared to Case 1 and Case 2. It may be noted that in the above three cases, Case 1 and Case 2 are non-dominated solutions and have lower fitness values.

The way the fitness function was defined, for a maximization problem, if the objective function value is large, the fitness value reduces while for a minimization problem also, the fitness value reduces if the objective function value is small. Solutions with lower fitness values are only kept for the next generation. Further, in the limit, when the objective functions to be maximized approach an infinite value and the objective functions to be minimized approach zero, in both the cases, the fitness value will be equal to zero.

In the optimization method, the solutions are first compared and selected based on their fitness function values. The inferior/dominated solutions are rejected and only the superior/non-dominated solutions are retained in the populations for the next generation. Further, in this study, for performing the non-dominated sorting, the solutions are compared in terms of their corresponding objective function values and not on the basis of the fitness function value.

6.6 Validation

Neither experimental nor simulation results are available for H_2O–LiCl operated double effect series and parallel configurations shown in Chapter 4 (Refer Fig. 4.1a and Fig. 4.1b). A similar double effect series configuration was however simulated earlier by Won and Lee [8] long back in 1991 with H_2O–LiCl for a wide range of operating temperatures, but the modelling procedure adopted in Ref. [8] was entirely different from the current study. In their modelling, Won and Lee [8] calculated the temperature in the LPG (which they referred as second stage generator (GC)) iteratively from mass balance starting with an assumed value of solution concentration at GC exit (X_{GC}). This LPG temperature was however not indicated in their paper, instead, X_{GC} was shown as output. Whereas in the current modelling, the LPG temperature is a model input parameter and the solution concentration at HPG exit (X_8) is assumed which is calculated iteratively until the LPG heat balance is satisfied [2, 3]. Moreover, the equations which were used for calculating thermodynamic properties of H_2O–LiCl in Ref. [9] are not same with the equations considered in the present study. On the other hand, the double effect configurations presented in Refs. [9, 10] for H_2O–LiCl are not similar with the ones shown in Chapter 4 (Refer Fig. 4.1a and Fig. 4.1b). Hence, the model validation for H_2O–LiCl was not possible in the series and parallel double effect configurations considered for this study. Model validation was however possible for the H_2O–LiBr operated double effect series flow type VARS. This was already done in Chapter 4 by comparing the results obtained from simulation of the double effect H_2O–LiBr series configuration with the previously published results of Gomri and Hakimi [2] and Farshi et al. [3]. Hence, these are not repeated again in this chapter.

6.7 Results and discussion

The optimal results of the H_2O–LiCl and H_2O–LiBr operated double effect series and parallel configurations are discussed separately in subsection 6.7.1 for the series and in subsection 6.7.2 for the parallel configuration. For both the system configurations, the optimal results are shown for four different cases of fixed condenser, absorber and evaporator temperatures (T_C, T_A and T_E). Case 1 corresponds to fixed component temperatures of $T_C = T_A = 33$°C and $T_E = 8$°C while Case 2 refers to fixed $T_C = T_A = 35$°C and $T_E = 8$°C. Similarly Case 3 and Case 4 are for fixed component temperatures of $T_C =$

T_A = 38°C and T_E = 8°C and $T_C = T_A$ = 35°C and T_E = 5°C respectively.

6.7.1 Optimized results of the double effect series configuration

The optimal combinations of T_{LPG} and T_{HPG} obtained for the H_2O–LiCl and H_2O–LiBr operated double effect series configurations, along with the optimized performance parameters, are listed in Table 6.2. For both H_2O–LiCl and H_2O–LiBr, more specifically, two sets of optimal results are shown against each case except for the Case 2, Case 3 and Case 4 where only one single set of optimal results is shown for the H_2O–LiCl system. This single set of solutions corresponding to H_2O–LiCl operated double effect series configuration during Case 2, Case 3 and Case 4 are in fact the optimal solutions for which the COP and exergy efficiency are the maximum and total irreversibility is the minimum. For the solutions with two sets of results, the first set of optimal results represent the states of operating conditions for maximum exergy efficiency (or minimum total irreversibility) while the second set of results corresponds to the condition of maximum COP. However, from the two sets of solutions, presented for each case, not much difference was seen, particularly in case of the optimal solutions obtained for the H_2O–LiCl operated double effect series configuration during Case 1. In fact, for H_2O–LiBr also, the difference between the two optimal decision parameters and the corresponding objective function values was not very significant. The optimal solutions were so close to each other that there were almost negligible differences which in fact in certain way ensure the correctness of the obtained optimal solutions. This is correct in the sense that the optimal solution corresponding to (i) maximum COP; (ii) maximum exergy efficiency (or minimum irreversibility) is almost a single solution. This is because conditions at which COP becomes the maximum should ideally also be the conditions corresponding to maximum exergy efficiency (or minimum total system irreversibility). Thus, the solutions which were shown in Table 6.2 are correct representations of what was obtained from optimization of the double effect series configuration with almost negligible difference among the optimal solutions. This however may not be the case always, as in some cases; the optimal conditions at which the COP becomes the maximum may not be the conditions corresponding to maximum exergy efficiency (or minimum total system irreversibility). As shown in Table 6.2, for the two sets of solution (in fact they are almost the same solution in both the sets), practically it may be difficult to maintain such a precision level, however from the results shown for various cases of

fixed condenser, absorber and evaporator temperatures, one can decide to operate the double effect H_2O–LiCl series configuration say for example at T_{LPG} =71°C and T_{HPG} =105°C to obtain optimum system performance during Case 1 at fixed $T_C = T_A$=33°C and T_E =8°C. Similarly, for the H_2O–LiBr series configuration during Case 1, the optimal T_{LPG} is 75°C and optimal T_{HPG} is 112°C.

It was mentioned earlier that in the optimization process, maximum 200 numbers of generations were considered which was also set as the terminating criteria. To show that it was not premature termination of the optimization algorithm, the variation of the fitness function value with numbers of generations is presented in Fig. 6.5 specifically for Case 1 at $T_C = T_A$=33°C and T_E =8°C for the H_2O–LiCl operated double effect series flow type VARS. The fitness function value reduces initially with number of generations and remains constant after certain number of generations without any further change thereafter. The same variations of fitness function value with numbers generations were observed in the other cases also with both H_2O–LiCl and H_2O–LiBr, hence these are not shown again and again.

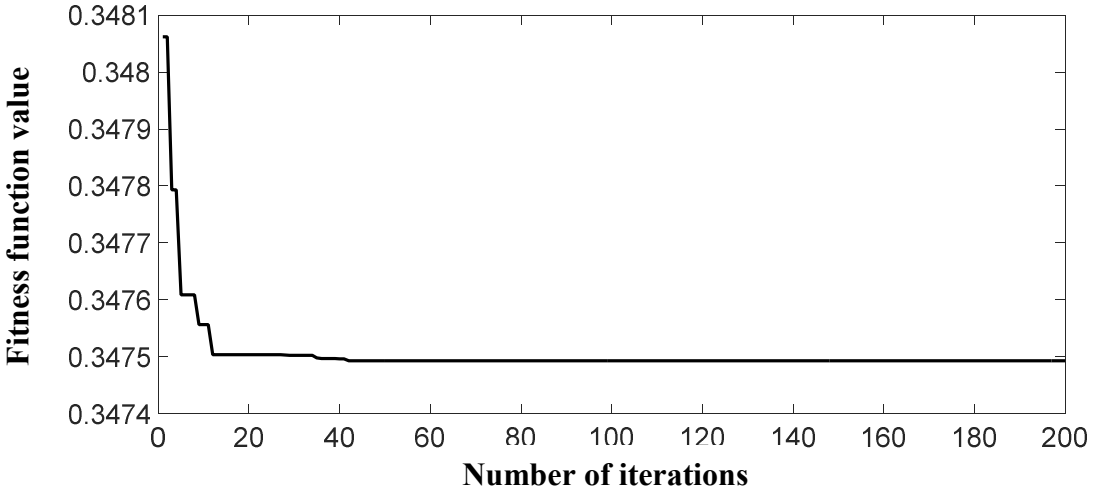

Fig. 6.5**:** Variation of fitness value with number of generations during optimization of the double effect series flow vapour absorption refrigeration system at $T_C = T_A$= 33°C and T_E=8°C with water-lithium chloride as solution pair.

From the results shown in Table 6.2, it is also visible that for a given case of fixed condenser, absorber and evaporator temperatures, the optimal T_{HPG} and T_{LPG} combinations are different for the two working fluid pairs. It was found that the performance of the double effect H_2O–LiCl series configuration is optimized at relatively

low T_{HPG} and T_{LPG} compared to those of the H_2O–LiBr system. Further it was seen that the optimum COPs of the H_2O–LiCl operated double effect series configuration are slightly lower than those of the H_2O–LiBr series configuration. Contrary to this, the optimum exergy efficiencies were more and the total system irreversibility values were less for the H_2O–LiCl system compared to those of H_2O–LiBr. This is certainly an operational advantage with H_2O–LiCl over H_2O–LiBr. From the optimum results presented in Table 6.2, it is also evident that both the H_2O–LiBr and H_2O–LiCl operated double effect series configurations perform better at lower T_C and T_A (and also at higher T_E).Therefore, highest optimum performance of the double effect H_2O–LiCl and H_2O–LiBr series flow configurations was obtained during Case 1.

In this work, the GA program was developed in such a way that the non-dominated PFs of the optimal solutions were obtained say for example as 1st set of best PF (PF1), 2nd set of best PF (PF2) and so on. Corresponding to system optimization during Case 1, three such best sets of trade-off solutions are shown in Fig. 6.6 (a–c) and Fig. 6.7 (a–c) in terms of (a) COP and total irreversibility rate (b) COP and exergy efficiency and (c) exergy efficiency and total irreversibility rate for both the double effect H_2O–LiCl and H_2O–LiBr series configurations. These Pareto optimal solutions shown in Figs. 6.6 and 6.7 are almost nearly equal to each other that vary within a very narrow range of values. The objective functions (COP, exergy efficiency and total irreversibility rate) are actually conflicting in nature. Say for example, COP cannot be increased by simultaneously reducing the total irreversibility. Simultaneous improvement of both the objectives is not possible; any increase in COP will always be accompanied by increase in irreversibility. This is clearly depicted in Figs. 6.6 and 6.7. In general, the Pareto diagrams are meant for showing the conflicting nature of the objective functions and certainly not for showing any trend of variation of the objectives with respect to change in the decision variables.

The PF1, shown in Figs. 6.6 and 6.7 contain the 1st best set of trade-off solutions in terms of COP, exergy efficiency and total system irreversibility. Additionally, PF2 and PF3 are also shown in Figs. 6.6 and 6.7. The points marked A and B in PF1 of Fig. 6.6 (a) correspond to the optimal results shown in Table 6.2 for the double effect H_2O–LiCl series flow system during Case 1. The point A corresponds to the set of solution with total irreversibility of 36.355 kW while the point B is for the other set of solution

corresponding to the total system irreversibility of 36.362 kW. As indicated earlier in Table 6.2 and also from Fig. 6.6 (a), it was seen that the COP values with respect to point A (1.431189**)** and point B (1.4312356**)** are almost nearly equal. However, since the COP at point B was slightly more (if considered up to all decimal places and an output of the computer program), therefore, the total system irreversibility corresponding to point B was also marginally high (7 Watt more than the irreversibility at point A). The corresponding Pareto optimal solutions are marked C and D in Fig. 6.6 (b) where the Pareto optimal solutions are shown in terms of COP and exergy efficiency. Although the difference was minimal, yet the exergy efficiency was slightly more at point C (22.078%) than its value at point D (22.074%). It was also seen that the optimal T_{HPG} and T_{LPG} combination at which the COP was maximized was not much different from the solution corresponding to maximum exergy efficiency.

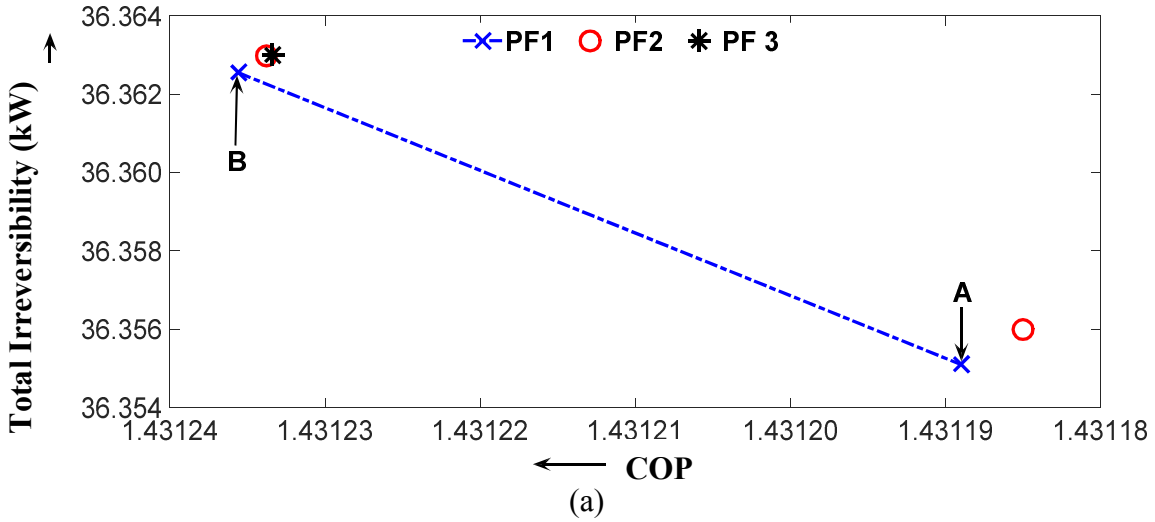

(a)

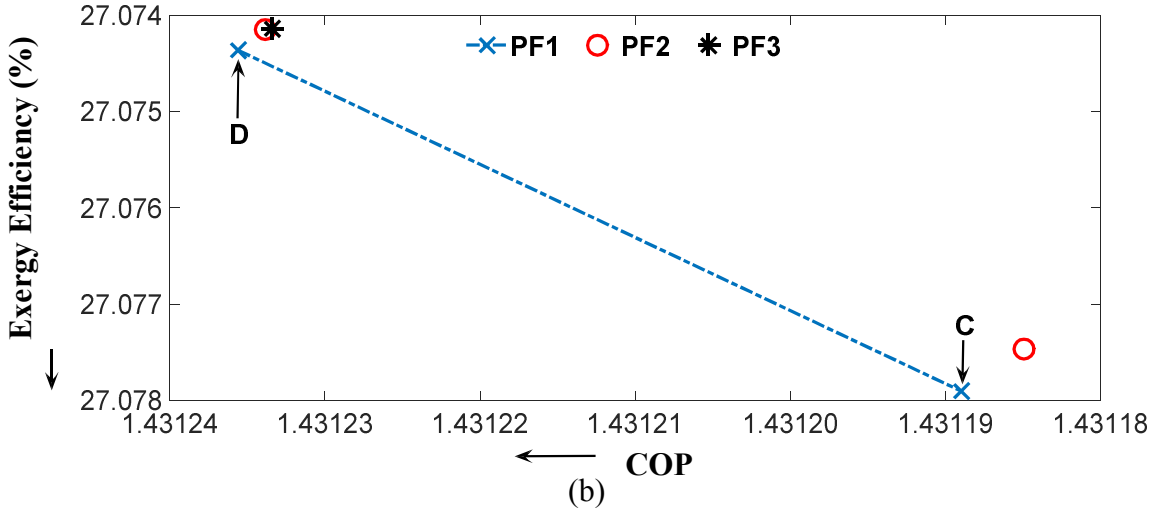

(b)

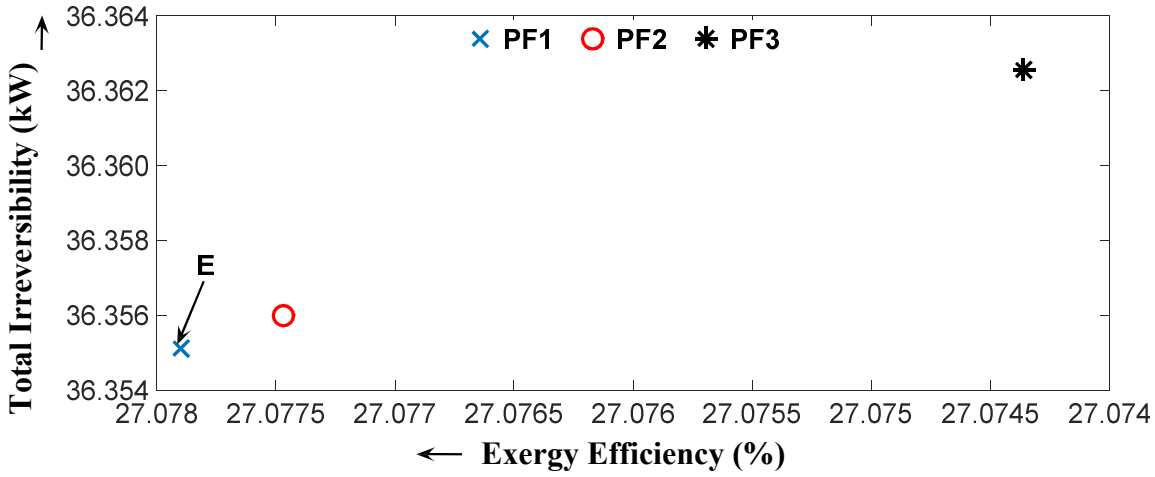

(c)

Fig. 6.6: The best three Pareto fronts in terms of (a) COP and total irreversibility (b) COP and exergy efficiency and (c) exergy efficiency and total irreversibility for the double effect H_2O–LiCl series configuration with respect to system optimization during Case 1 at $T_C = T_A = 33°C$ and $T_E = 8°C$

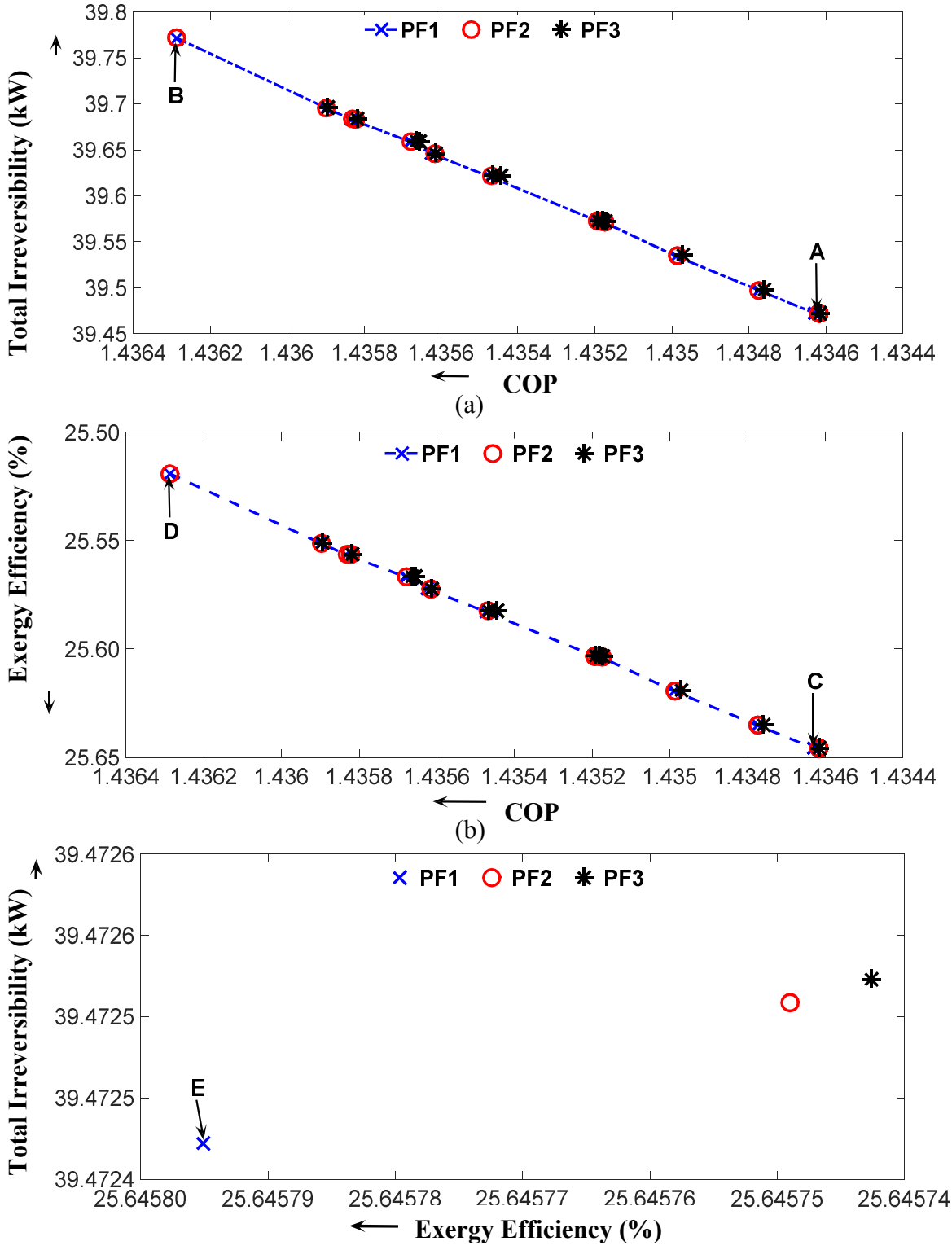

Fig. 6.7: The best three Pareto fronts in terms of (a) COP and total irreversibility (b) COP and exergy efficiency and (c) exergy efficiency and total irreversibility for the double effect H_2O–LiBr series configuration with respect to system optimization during Case 1 at $T_C = T_A = 33°C$ and $T_E = 8°C$

These are in fact two solutions very close to each other and therefore, can be considered as a single optimal solution corresponding to maximum COP and maximum exergy efficiency (also minimum irreversibility).

During system optimization with the help of GA, the optimal solutions (parameter values) were obtained in such a way that if there was a single best solution which is not dominated by other comparatively good solutions, then it was marked as a single point in the PF. The Pareto solutions shown in Fig. 6.6 (c) are three such single point solutions. The point E corresponds to the solution that was represented by point A in Fig. 6.6 (a) and point C in Fig. 6.6 (b). The other two single Pareto optimal solutions shown in Fig. 6.6 (c) are the solutions of PF2 and PF3 respectively. As can be seen, all these Pareto optimal solutions were nearly equal and hence, the identified optimal values of T_{LPG} and T_{HPG} can be chosen for obtaining optimum performance from the double effect H_2O–LiCl series flow configuration at $T_C = T_A$ = 33°C and T_E = 8°C. Further it can be mentioned that although total irreversibility is conflicting separately with COP and exergy efficiency as it was shown in Figs. 6.6 (a) and (b), but the exergy efficiency and the total irreversibility as objective functions are not conflicting. This is evident from the single optimal solution appearing in PF1, PF2 and PF3 of Fig. 6.6 (c).

Similarly, the PFs, depicting the conflicting nature of the objective functions corresponding to optimization of the double effect H_2O–LiBr series flow VARS are shown in Figs. 6.7 (a–b) for Case 1. The points marked A and B in PF1 of Fig. 6.7 (a) correspond to the first and second set of results in Table 6.2 for Case 1. The points C and D in Fig. 6.7 (b) are identical with the solutions A and B in Fig. 6.7 (a). The solution corresponding to point B in Fig. 6.7 (a) and point D in Fig. 6.7 (b) is the point E in Fig. 6.7 (c). The single optimal solution appearing in PF1, PF2 and PF3 of Fig. 6.7 (c) is representative of the fact that the exergy efficiency and the total irreversibility rate as objective functions are not conflicting in nature. The PFs can also be shown for the other cases, however this will unnecessarily increase the length of the paper, hence, these are not shown and instead, for the other cases, the best solutions corresponding to PF1 are shown in Table 6.2.

During optimization of the double effect VARSs, in addition to T_{LPG} and T_{HPG}, the condenser, absorber and evaporator temperatures could also have been considered as decision variables by specifying their lower and upper limits. However, this was not

done because this is known that a VARS always performs better at low condenser and low absorber temperature while it provides superior performance at higher evaporator temperature. Therefore, even if these temperatures had been considered as decision variables, the optimized solutions would have been obtained at the lower limit of the condenser (also absorber) temperature and the upper limit of the evaporator temperature. For this reason, these were not considered as decision variables and instead, the optimization was done separately for four different cases of fixed condenser, absorber and evaporator temperatures taking only T_{LPG} and T_{HPG} as decision variables.

The irreversible losses (irreversibility) occurred in various components of the H_2O–LiCl and H_2O–LiBr operated double effect series configurations at the optimized conditions are shown in Table 6.3 for various cases with respect to the first set of results corresponding to minimum irreversibility and maximum exergy efficiency. It was seen that except in the SHE I during Case 3 and Case 4 and in the HPG during Case 1 and Case 4, in all other components, the irreversible losses were less for the H_2O–LiCl double effect series configuration compared to those of the H_2O–LiBr system. Mainly it was the irreversibility in the absorber that was responsible for the difference in total irreversibility of the two systems. Therefore, in all the cases, the total irreversibility rate was less for the H_2O–LiCl operated double effect series configuration compared to that of the H_2O–LiBr system.

Table 6.2: Optimal combinations of T_{LPG} and T_{HPG} and the optimized COP, exergy efficiency and total system irreversibility obtained for various cases of fixed component temperatures with H_2O–LiCl and H_2O–LiBr as solution pairs in the double effect series configuration.

Cases	H_2O–LiCl					H_2O–LiBr				
	T_{LPG} (°C)	T_{HPG} (°C)	COP (max)	η(%)(max)	$\dot{I}_{tot}$(kW) (min)	T_{LPG} (°C)	T_{HPG} (°C)	COP (max)	η (%)(max)	$\dot{I}_{tot}$(kW) (min)
Case 1	71.24	104.75	1.431	27.078	36.355	74.71	111.67	1.435	25.646	39.472
	71.25	104.77	1.431	27.074	36.362	75.30	112.46	1.436	25.519	39.772
Case 2	73.54	109.23	1.378	25.110	40.715	80.61	121.03	1.400	23.356	45.277
						81.12	121.72	1.401	23.264	45.538
Case 3	76.96	115.82	1.253	21.698	50.118	89.56	135.13	1.353	20.613	53.928
						89.98	135.69	1.353	20.556	54.137
Case 4	73.54	112.36	1.234	21.943	49.297	86.42	132.09	1.352	20.983	52.615
						86.86	132.69	1.353	20.918	52.844

Table 6.3: The irreversible losses occurring in different VARS components (except LPG where irreversibility is almost negligible) of the double effect series configuration with respect to the first set of results in Table 6.2 corresponding to minimum irreversibility and maximum exergy efficiency for both the working fluid pairs during various test cases

Component irreversibility (kW)	Case 1		Case 2		Case 3		Case 4	
	H_2O–LiCl	H_2O–LiBr	H_2O–LiCl	H_2O–LiBr	H_2O–LiCl	H_2O–LiBr	H_2O–LiCl	H_2O–LiBr
HPG	7.007	6.887	6.951	7.021	7.216	7.277	7.432	7.352
EVA	5.838	5.838	5.838	5.838	5.838	5.838	9.841	9.841
COND	3.518	3.619	4.695	4.848	6.505	6.684	4.779	4.958
ABS	13.650	16.298	15.431	20.064	18.593	25.670	14.446	21.827
SHE I	2.040	2.331	2.540	2.562	4.117	2.841	4.398	2.904
SHE II	2.988	3.078	3.777	3.289	6.129	3.554	6.655	3.638
ExVs	1.303	1.385	1.453	1.618	1.697	2.022	1.694	2.047
SP	0.012	0.037	0.028	0.036	0.023	0.041	0.052	0.048
Total	36.355	39.472	40.715	45.277	50.118	53.928	49.297	52.615

Although, the COP was marginally low for H_2O–LiCl at the optimized conditions but certainly the performance of the H_2O–LiCl operated double effect series configuration was superior in terms of lower total system irreversibility and higher exergy efficiency. This speaks about suitability of H_2O–LiCl for use in double effect VARS at relatively low LPG and HPG temperatures. In fact, it would not be possible to operate the double effect H_2O–LiCl VARS at higher T_{HPG} and T_{LPG} ; the solution concentration will exceed 50% limit leading to crystallization of the salt solution. With H_2O–LiBr, it is however possible to operate the double effect VARS avoiding crystallization relatively at higher T_{HPG} and T_{LPG} . In fact, the double effect H_2O–LiBr system provides better performance at relatively higher T_{HPG} and T_{LPG} . If the H_2O–LiBr system is made to operate at the same optimal T_{HPG} and T_{LPG} corresponding to H_2O–LiCl, it would perform low compared to that of the H_2O–LiCl system.

6.7.2 Optimized results of the double effect parallel configuration

For the double effect parallel configuration, the optimal combinations of D, T_{LPG} and T_{HPG} obtained for various cases of fixed absorber, condenser and evaporator temperatures are shown separately for the two working fluid pairs in Table 6.4. For some cases, two best sets of solutions were found with respect to (i) maximum COP and (ii) maximum exergy efficiency (or minimum total irreversibility rate) while for some other cases, only a single set of solutions were obtained with H_2O–LiCl. Cases for which two best sets of solutions are shown, the first set corresponds to the optimal operating conditions of maximum exergy efficiency (or minimum total irreversibility) while the second set of results represent the operating conditions corresponding to maximum COP.

Table 6.4: Optimal combinations of D, T_{LPG} and T_{HPG} and the optimized COP, exergy efficiency and total system irreversibility obtained for various cases of fixed component temperatures with H_2O–LiCl and H_2O–LiBr as solution pairs in the double effect parallel configuration.

Cases	H_2O–LiCl						H_2O–LiBr					
	$D(\%)$	T_{LPG} (°C)	T_{HPG} (°C)	COP (max)	η (%)(max)	$\dot{I}_{tot}$(kW) (min)	$D(\%)$	T_{LPG} (°C)	T_{HPG} (°C)	COP (max)	η (%)(max)	$\dot{I}_{tot}$(kW) (min)
Case 1	46.67	67.73	105.19	1.468	27.663	35.067	47.32	69.17	108.91	1.464	26.759	36.906
	48.99	68.66	105.81	1.469	27.559	35.360	41.65	69.95	114.53	1.477	25.831	38.629
Case 2	53.22	72.75	110.51	1.423	25.674	39.430	44.33	73.47	117.96	1.430	24.375	42.289
	54.93	73.43	110.89	1.424	25.613	39.577	40.79	74.45	122.90	1.440	23.716	43.763
Case 3	56.27	76.94	116.50	1.316	22.677	47.171	42.43	78.58	126.61	1.361	21.862	49.326
							42.43	81.79	134.77	1.387	21.188	51.475
Case 4	56.36	73.52	112.91	1.300	23.021	46.134	41.13	77.02	129.03	1.377	21.790	49.436
							46.11	81.31	134.59	1.388	21.224	51.544

The cases for which only one set of best results was found, the single set of solution corresponds to maximum COP, maximum exergy efficiency and minimum total irreversibility. Unlike in the H_2O–LiCl series configuration, where the difference in optimal T_{LPG} and T_{HPG} values was very less, in the H_2O–LiCl parallel configuration however, at least for Case 1 and Case 2, there exist some differences between the optimal solutions corresponding to maximum COP and maximum exergy efficiency (or minimum total irreversibility rate). This was mainly due to D and T_{LPG} values corresponding to maximum COP and maximum exergy efficiency which in the H_2O–LiCl parallel configuration were slightly different for Case 1 and Case 2. For Case 3 and Case 4, however, a single set of optimal solutions was obtained for the H_2O–LiCl parallel configuration. Contrary to this, in the H_2O–LiBr parallel configuration, the optimal D, T_{LPG} and T_{HPG} values corresponding to maximum COP and maximum exergy efficiency (also minimum irreversibility) were somewhat different. For such cases where the optimal operating conditions corresponding to maximum COP and maximum exergy efficiency (or minimum irreversibility) are different, either of the two conditions be selected depending on criteria based on the maximum exergy efficiency (or minimum total irreversibility) or the maximum COP. Say for example, the COP value in the H_2O–LiBr parallel configuration at optimal condition of maximum exergy efficiency (also minimum irreversibility) corresponding to Case1 is 0.88% less compared to 3.59% increase in exergy efficiency and 4.46% reduction in total irreversibly from condition of maximum COP. Therefore, the condition of maximum exergy efficiency (or minimum irreversibility) be preferred for this Case 1 where T_{HPG} and T_{LPG} combinations were little different for maximum COP and maximum exergy efficiency (also minimum irreversibility).

From the results in Table 6.4, again it was seen that the optimal combinations of D, T_{HPG} and T_{LPG} were different for the two working fluid pairs. The optimal values of the decision parameters were also different for different cases of fixed condenser, absorber and evaporator temperatures. It was found that the optimal D was relatively high for the H_2O–LiCl system compared to H_2O–LiBr in all the four test cases. Further, the optimal T_{LPG} and T_{HPG} values were found to be low for the H_2O–LiCl system compared to those for the H_2O–LiBr, particularly the optimal HPG temperatures were significantly low. Earlier in the H_2O–LiCl series configuration, for various test cases, the

optimal T_{LPG} and T_{HPG} values were found to be low compared to their corresponding optimal T_{LPG} and T_{HPG} values in the H_2O–LiBr system. However, in the parallel configuration, not much difference was seen between the optimal T_{LPG} values. Like in the series configuration, in the parallel also, the optimized COP values were slightly lower for the H_2O–LiCl system than those of the H_2O–LiBr system in various test cases. But on the other hand, the optimized exergy efficiencies were more and the optimized total irreversibility rates were less for H_2O–LiCl than their H_2O–LiBr counterparts. Exceptionally in Case 1, with respect to the first set of optimal solutions of Table 6.4 corresponding to maximum exergy efficiency, it was observed that the performance of the H_2O–LiCl parallel configuration was not only better in terms of higher exergy efficiency and lower total irreversibility but also superior to the H_2O–LiBr counterpart in terms of slightly higher COP.

It was also observed that for H_2O–LiCl, the optimal D values during various test cases changed from 46.67% to 56.36% while for H_2O–LiBr, the range of D variation was narrow from 40.79% to 47.93%. In case of H_2O–LiCl however, the optimum D value was relatively less at lower and more at higher condenser and absorber temperatures. Further, the optimum D also increased with decrease in the evaporator temperature. Again for both the working solution pairs, the optimized performance of the double effect parallel flow configuration was the best during Case 1 at $T_C = T_A = 33$°C and $T_E = 8$°C.

The first three PFs of optimal solutions obtained during Case 1 for the double effect H_2O–LiCl parallel configuration, showing the conflicting nature between (a) COP and total irreversibility and (b) COP and exergy efficiency are shown in Fig. 6.8 (a–b). The PF1, shown in Figs. 6.8 (a) and (b) contain the 1st best set of Pareto optimal solutions. It was seen that the number of Pareto optimal solutions appearing in PF1, PF2 and PF3 of Fig. 6.8 (a) is comparatively more. Total 27 solutions appeared in PF1 and compared to the solutions shown in the other PFs, these were comparatively better solutions. Further it was seen that for all these solutions, the corresponding objective function values were not much different. The point A in PF1 of Fig. 6.8 (a) corresponds to the 1stset of solutions shown in Table 6.4 for Case1 corresponding to the maximum exergy efficiency (27.663%) and the minimum total irreversibility (35.067 kW) while the point B is for the 2nd set of solution corresponding to maximum COP (1.469) with

relatively higher total system irreversibility (35.360 kW). Therefore, although the COP at point B was slightly higher, but the solution corresponding to point A could be a better choice because the total irreversibility is the minimum at this point for almost same value of COP at points A and B.

The PFs obtained during Case 1 for the double effect H_2O–LiCl parallel configuration are presented in Fig. 6.8 (b) for showing the conflicting nature between COP and exergy efficiency. This time, total 32 solutions appeared in PF1 and again, all these optimal solutions were not much different and hence, the corresponding objective function values were also very close to each other. The points C and D appearing in PF1 are identical to points A and B of Fig. 6.8 (a). As such, although the differences in the objective function values were small, but the solution corresponding to point C is comparatively a better solution.

Similarly, the PFs obtained during Case 1 for the double effect H_2O–LiCl parallel configuration are presented in Fig. 6.8 (c). As can be seen in Fig. 6.8 (c), only one optimal solution was appearing in PF1, PF2 and PF3 and hence, it confirms the fact that the exergy efficiency and the total irreversibility rate as objective functions are not conflicting in nature. An increase in exergy efficiency is always accompanied by proportional decrease in the total irreversibility rate and vice versa. The point E marked in Fig. 6.8 (c) is the optimal solution corresponding to the point A of Fig. 6.8 (a) and C of Fig. 6.8 (b) respectively.

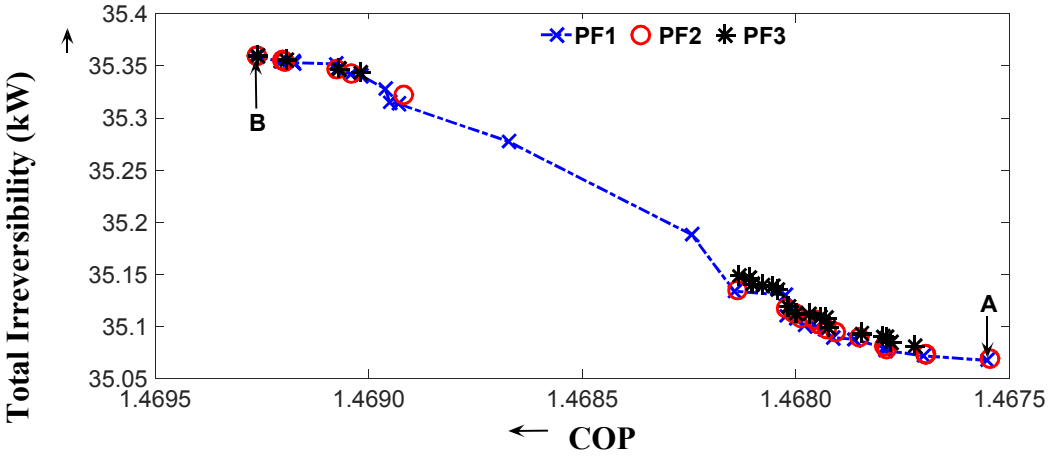

(a)

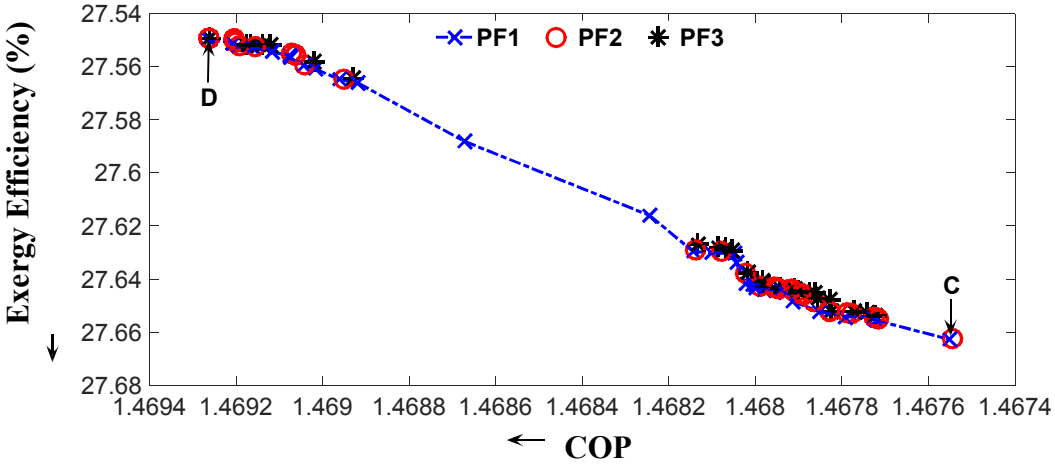

(b)

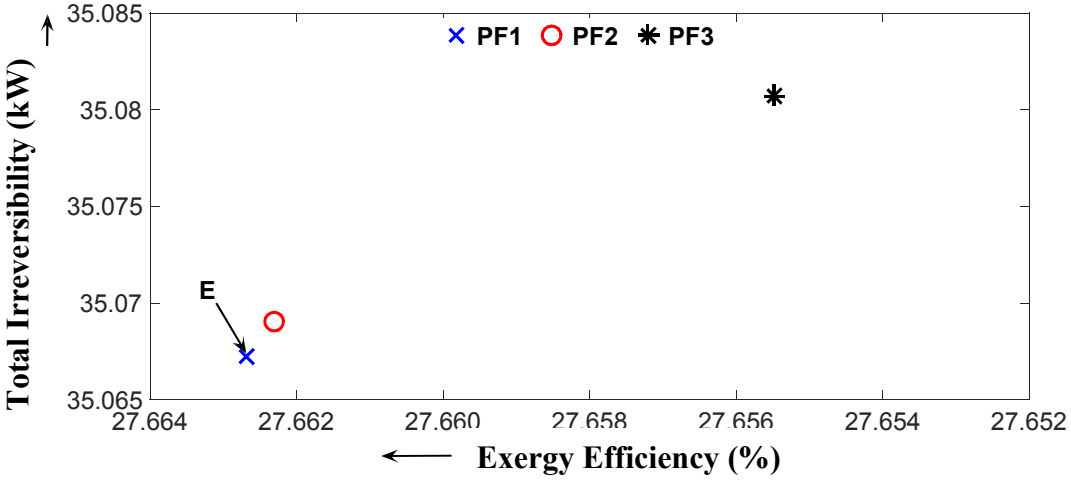

(c)

Fig. 6.8: The best three Pareto fronts in terms of (a) COP and total irreversibility (b) COP and exergy efficiency and (c) exergy efficiency and total irreversibility for the double effect H_2O–LiCl parallel configuration with respect to system optimization during Case 1 at $T_C = T_A = 33°C$ and $T_E = 8°C$

Hence, it represents the first set of solutions shown in Table 6.4 obtained during Case 1 for the H_2O–LiCl double effect parallel system.

Again for H_2O–LiBr, the Pareto optimal solutions obtained during Case 1 for the double effect parallel configuration are shown in Figs. 6.9 (a–c). The first set of Pareto front containing 18 optimal solutions in terms of COP and total irreversibility is shown in Fig. 6.9 (a). The points marked A and B in PF1 of Fig. 6.9 (a) correspond to the first and second set of results shown in Table 6.4 for H_2O–LiBr (Case 1). The points C and D in Fig. 6.9 (b) are the same optimal solutions represented by points A and B in Fig. 6.9 (a). The solution corresponding to point A in Fig. 6.9 (a) and point B in Fig. 6.9 (b) is represented by point E in Fig. 6.9 (c).

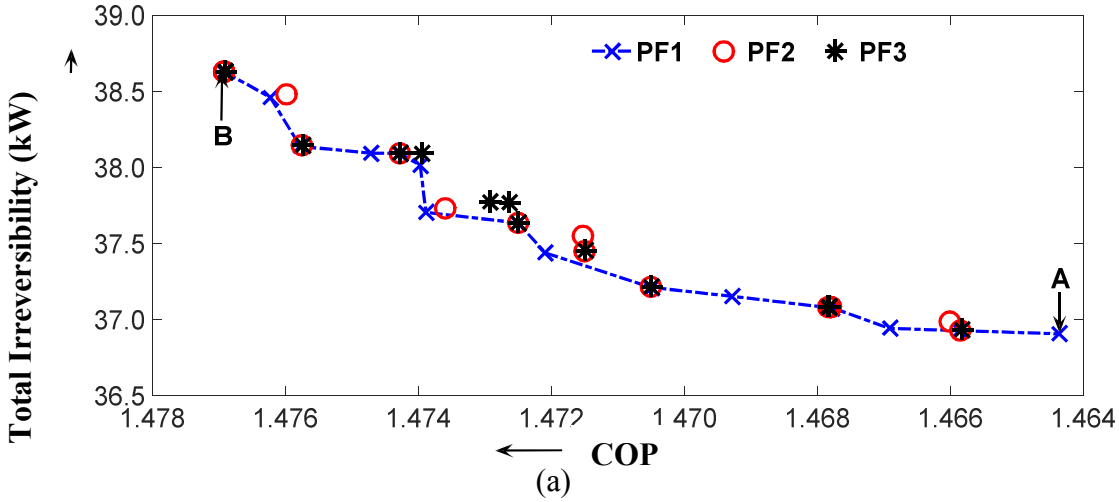

(a)

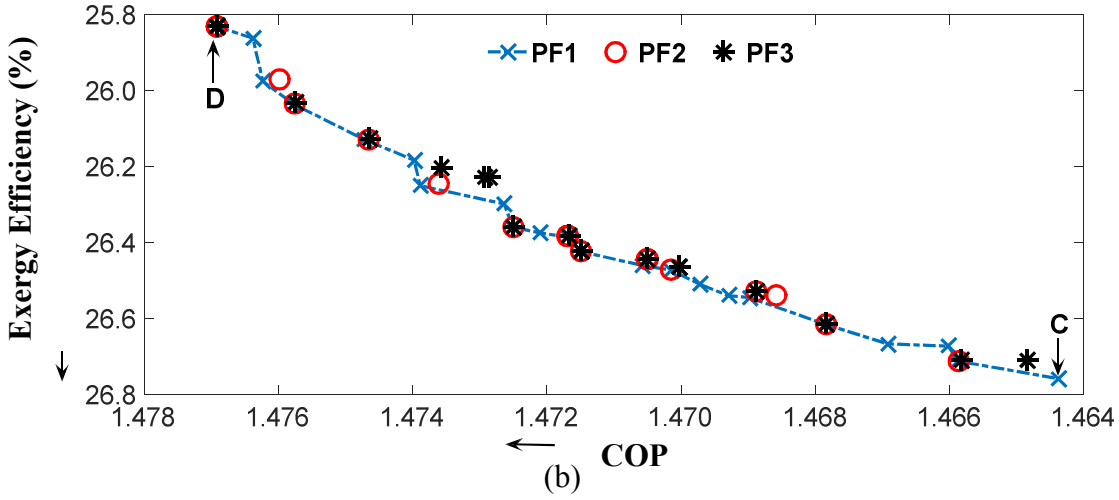

(b)

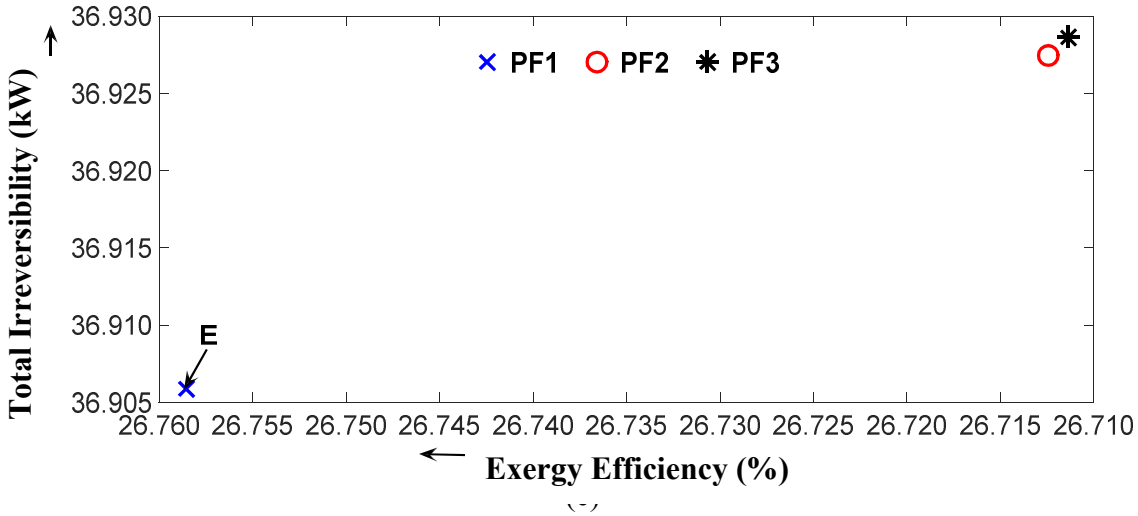

Fig. 6.9: The best three Pareto fronts in terms of (a) COP and total irreversibility (b) COP and exergy efficiency and (c) exergy efficiency and total irreversibility for the double effect H_2O–LiBr parallel configuration with respect to system optimization during Case 1 at $T_C = T_A$ =33°C and T_E = 8°C

Further to ensure the correctness of the reported optimal results, the program was run for a number of times and it was observed that during each run, almost, the same values of optimal results were obtained for both the series and parallel flow systems with H_2O–LiCl and H_2O–LiBr as solution pairs. For instance, the following sets of optimal results (Table 6.5) were obtained during three different runs while carrying out the optimization of the H_2O–LiCl operated double effect series flow type VARS. It was observed that the difference among the three sets of solutions was almost negligible and hence it was decided to show the optimal solution obtained during Run 1. Moreover, the optimal results corresponding to Run 1 and Run 3 were same.

Table 6.5**:** Optimal combinations of T_{LPG} and T_{HPG} and the optimized COP, exergy efficiency and total system irreversibility obtained during optimization of the H_2O–LiCl operated double effect series configuration at $T_C = T_A = 33$°C and $T_E = 8$°C.

Case	T_{LPG} (°C)	T_{HPG}(°C)	COP (max)	η(%) (max)	$\dot{I}_{tot}$(kW) (min)
Run1	71.24	104.75	1.431	27.078	36.355
Run2	71.25	104.77	1.431	27.074	36.363
Run3	71.24	104.75	1.431	27.078	36.355

6.7.3 Comparison of optimized results between series and parallel configuration

From the discussion presented in the previous sections, it was not clear as to how the performance of the double effect series and parallel systems varies at the optimized conditions. In this section, the optimized COP, exergy efficiency and total system irreversibility are compared for the series and parallel double effect VARS configurations. The comparison is shown for all the four cases and also for both the H_2O–LiCl and H_2O–LiBr solution pairs. The optimized COPs of the H_2O–LiCl and H_2O–LiBr operated double effect VARS configurations (series and parallel) are shown in Fig. 6.10 for various test cases. For both the solution pairs, the optimized COPs in various test cases were more in the parallel configuration compared to those for the series configuration. Further, the optimized COPs were slightly less for H_2O–LiCl compared to those of H_2O–LiBr in both the series and parallel configurations except in Case 1 where the COP of the double effect H_2O–LiCl parallel configuration at optimized condition of minimum irreversibility (on maximum exergy efficiency) was marginally

higher than its H_2O–LiBr counterpart. At optimized conditions of maximum COP, the COPs of the H_2O–LiCl systems were however always lower than those of H_2O–LiBr.

Similarly, the comparison of exergy efficiency at optimized conditions between the series and parallel configuration for various test cases is shown in Fig. 6.11. The optimized exergy efficiencies in various test cases were slightly higher in the parallel configuration compared to those of the series for both the solution pairs**.** Consequently, for both the solution pairs, the total system irreversibility rates were also comparatively less in the parallel configuration compared to those in the series configuration (Fig. 6.12). The irreversible losses occurring in the major VARS components during Case 1 at the optimized conditions are shown in Fig. 6.13. These are shown for both the series and parallel configurations and also separately for the H_2O–LiCl and H_2O–LiBr solution pairs. The HPG irreversibility in the double effect parallel configuration was more compared to that of the series in both the H_2O–LiCl and H_2O–LiBr operated systems. The evaporator irreversibility was the same in the series as well as parallel configuration for both H_2O–LiCl and H_2O–LiBr. In the condenser, the irreversibility rate was slightly less in the parallel configuration for both H_2O–LiCl and H_2O–LiBr compared to those in the series configuration. Irreversible losses in the LPG, SP and the expansion valves were very less; hence the losses occurring in these components are not shown in Fig. 6.13.

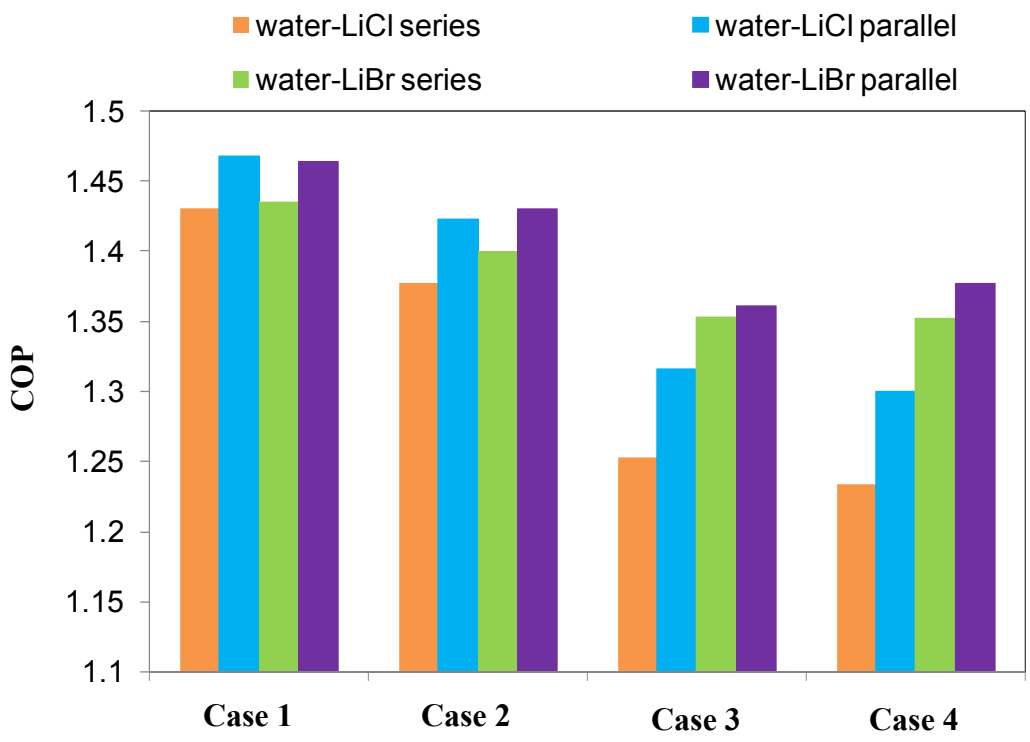

Fig. 6.10: The optimized COPs of the H_2O–LiCl and H_2O–LiBr operated double effect series and parallel configurations during various test cases

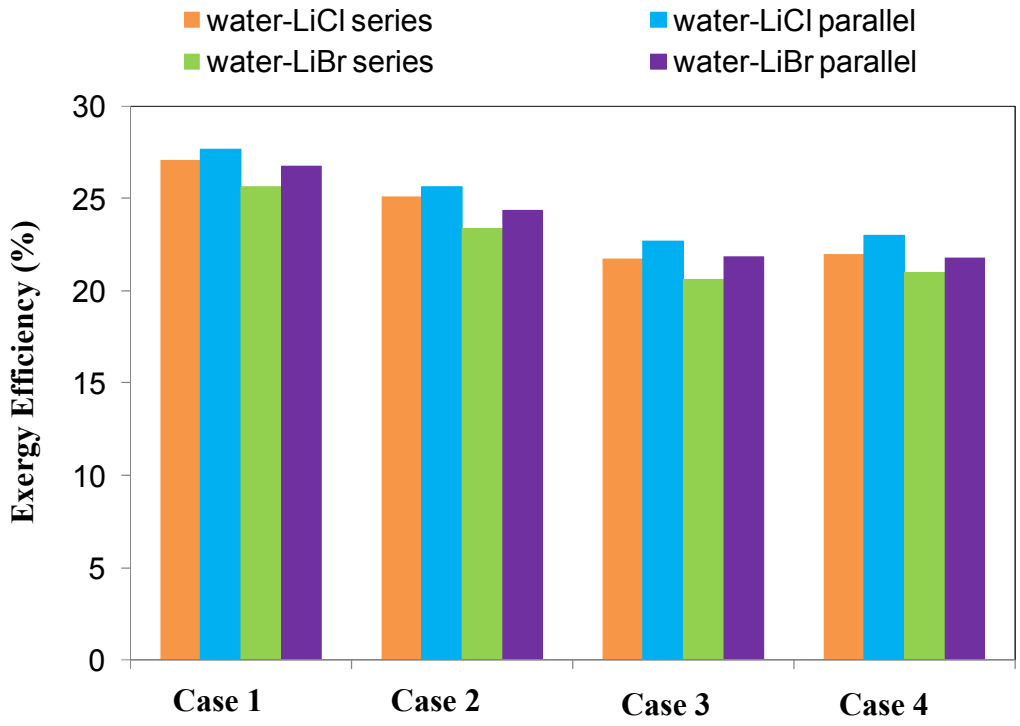

Fig. 6.11: The optimized exergy efficiencies of the H_2O–LiCl and H_2O–LiBr operated double effect series and parallel configurations during various test cases

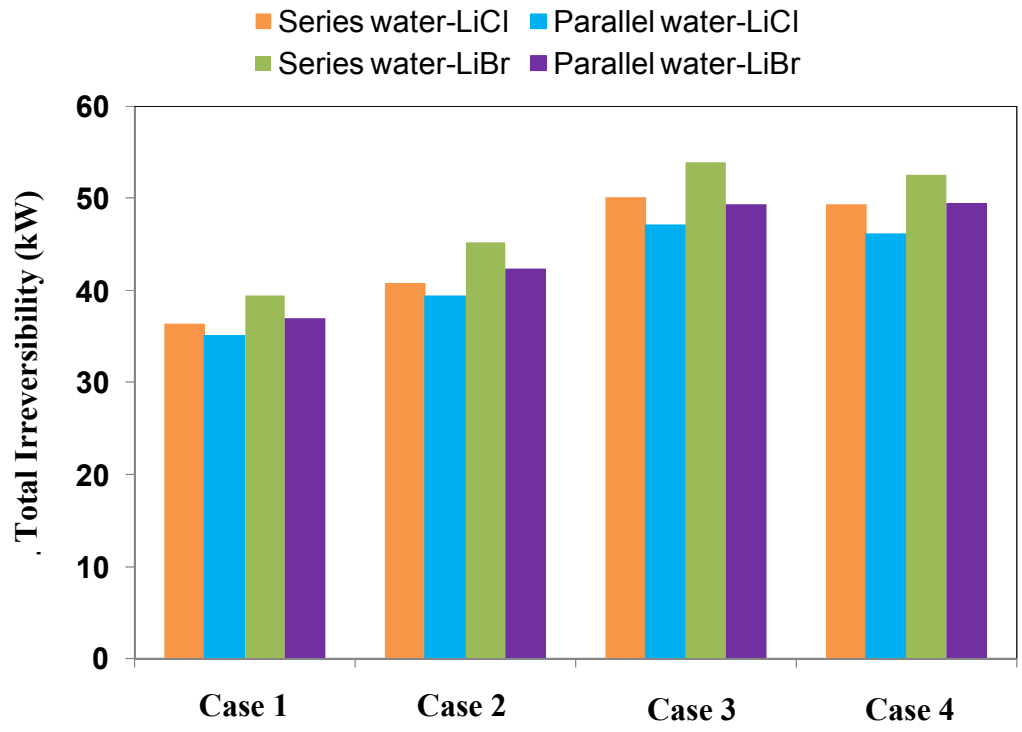

Fig. 6.12: The optimized total irreversibility values of the H_2O–LiCl and H_2O–LiBr operated double effect series and parallel configurations during various test cases

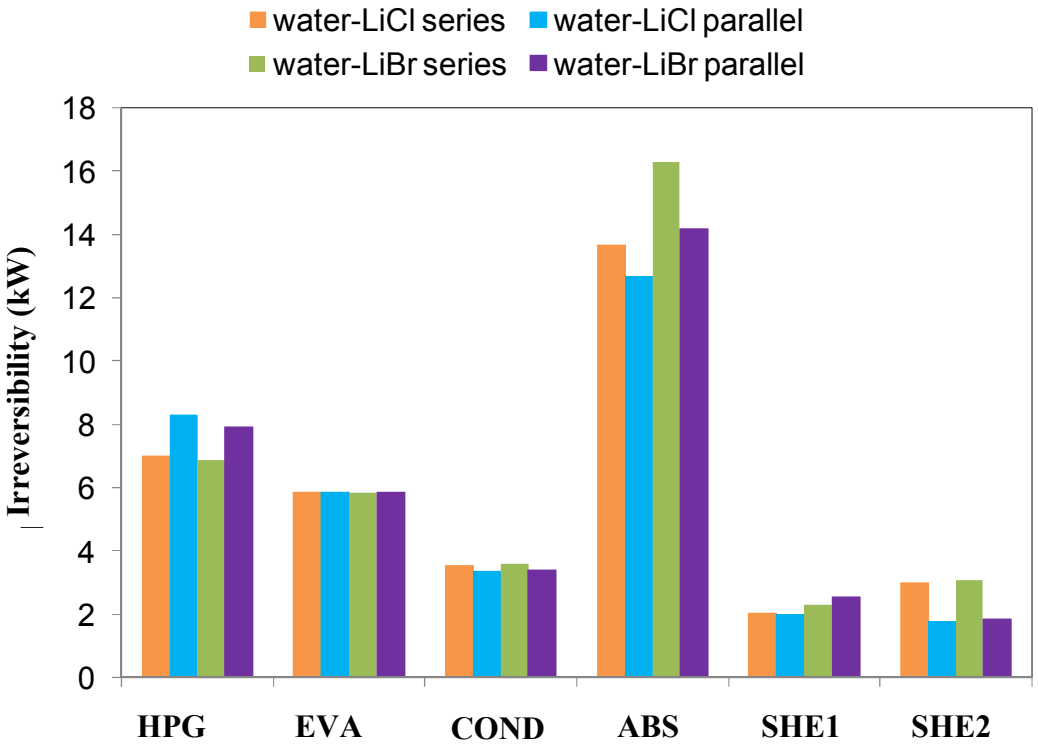

Fig. 6.13: The irreversible losses occurring in the major VARS components during Case 1 at the optimized operating conditions

But overall, the total system irreversibility rate was less for the parallel configuration for both the H_2O–LiCl and H_2O–LiBr solution pairs. This was mainly due to reduction of irreversibility rate in the condenser, SHE II and particularly in the absorber.

Further, between the H_2O–LiCl and H_2O–LiBr operated double effect series and parallel configurations, it was seen that except in the HPG, in all other components and particularly in the absorber, the irreversible losses were significantly less for H_2O–LiCl compared to those with H_2O–LiBr. Therefore, in both the double effect series and parallel configurations, the total system irreversibility was less for H_2O–LiCl compared to its H_2O–LiBr counterpart. The evaporator irreversibility was however the same for both H_2O–LiCl and H_2O–LiBr in the series as well as in the parallel configuration.

6.7.4 Comparison of optimized results with those presented in Chapters 4 and 5

Through the optimization work presented in this Chapter, it was attempted to overcome some limitations which were faced during parametric analyses in Chapter 4 and Chapter 5. While comparing the optimized results with those presented in Chapter 4 and 5 it was found that almost similar results could be obtained from this GA based optimization study with what was reported in Chapters 4 and 5 for the H_2O–LiCl operated double effect series VARS configuration. The following table (Table 6.6) presents the comparison between what was obtained in this optimization study with the results presented in Chapters 4 and 5 for the double effect series configuration with H_2O–LiCl as working fluid. As can be seen in Table 6.6, for all the four cases, the optimal T_{LPG} and T_{HPG} values obtained in this study almost tallies with the values reported in preceding Chapters 4 and 5. During parametric analysis in Chapters 4 and 5, these parameters (T_{LPG} and T_{HPG}) were incremented by 1°C and therefore, T_{LPG} and T_{HPG} values were obtained accordingly and in this GA based optimization study also, almost similar values were obtained. However during optimization, since the optimal decision parameters were obtained following a series of GA operations from within the given lower and upper bounds of the parameters, therefore, optimal results were obtained in decimal values.

Similarly for the H_2O–LiCl operated double effect parallel VARS configuration, earlier in Chapters 4 and 5, the distribution ratio *'D'* was kept fixed at 50% for all the

cases and D was not reduced below 50% as it resulted in increase of solution concentration above 50%. This was realized as one of the limitations during the parametric analysis of the parallel system in finding out the optimum D, T_{LPG} and T_{HPG}. It was possible to find out the optimal combinations of D, T_{LPG} and T_{HPG} more precisely from this GA based optimization study and this is evident from the comparison shown in Table 6.7. Thus, this optimization study helped in overcoming the difficulties which were faced during parametric analysis in Chapters 4 and 5.

It may however be mentioned here again that there was a slight mismatch in T_{HPG} and T_{LPG} values corresponding to maximum COP and maximum exergy efficiency (also minimum irreversibility) during Case 1 which was found from parametric analysis in Chapters 4 and 5 for the double series and parallel VARS configurations. In case of the series configuration, although, the COP was maximum (1.428) at T_{LPG}=71ºC and T_{HPG} =105ºC, but the maximum exergy efficiency (29.26%) and the minimum irreversibility (36.32 kW) were found at T_{LPG}=69ºC and T_{HPG}=103ºC with a corresponding COP of 1.41. In case of the parallel configuration also, the operating conditions corresponding to maximum COP and maximum exergy efficiency were found to be slightly different in Chapters 4 and 5. Maximum COP (1.469) was found at T_{LPG}=69ºC and T_{HPG}=106ºC with a corresponding exergy efficiency of 27.5% and irreversibility of 35.48 kW (refer Table 6.7). But the maximum exergy efficiency (27.56%) with a corresponding minimum irreversibility (35.35 kW) and comparatively lesser COP (1.460) was actually found at T_{LPG}=68ºC and T_{HPG}=105ºC. Therefore this comes out to be clear cut case where the operating conditions corresponding to maximum COP were not the same with conditions corresponding to maximum exergy efficiency (or minimum total system irreversibility). This was the reason that the problem was solved as a multi objective optimization problem as there was uncertainty, although in some cases, it led to a single optimized solution due to the nature of the optimization problem with the given constraints.

Table 6.6: Comparison of optimal T_{LPG} and T_{HPG} and the optimized COP, exergy efficiency and total system irreversibility presented in this study with those of Chapters 4 and 5 for the double effect series configuration with H_2O–LiCl as working fluid.

Case	Results from optimization study					Results from Chapters 4 and 5				
	T_{LPG} (°C)	T_{HPG} (°C)	COP (max)	η(%) (max)	$\dot{I}_{tot}$(kW) (min)	T_{LPG} (°C)	T_{HPG} (°C)	COP (max)	η(%) (max)	$\dot{I}_{tot}$(kW) (min)
$T_C = T_A = 33$°C, $T_E = 8$°C	71.24	104.75	1.431	27.078	36.355	71	105	1.428	26.96	36.59
$T_C = T_A = 35$°C, $T_E = 8$°C	73.54	109.23	1.378	25.11	40.715	73	109	1.369	25.00	41.04
$T_C = T_A = 38$°C, $T_E = 8$°C	76.96	115.82	1.253	21.698	50.118	76	116	1.207	20.88	52.80
$T_C = T_A = 35$°C, $T_E = 5$°C	73.54	112.36	1.234	21.943	49.297	73	112	1.208	21.54	50.57

Table 6.7: Comparison of optimal T_{LPG} and T_{HPG} and the optimized COP, exergy efficiency and total system irreversibility presented in this study with those of Chapters 4 and 5 for the double effect parallel configuration with H_2O–LiCl as working fluid.

Case	Results from optimization study						Results from Chapters 4 and 5					
	D (%)	T_{LPG} (°C)	T_{HPG} (°C)	COP (max)	η(%) (max)	$\dot{I}_{tot}$(kW) (min)	D (%)	T_{LPG} (°C)	T_{HPG} (°C)	COP (max)	η(%) (max)	$\dot{I}_{tot}$(kW) (min)
$T_C = T_A = 33$°C, $T_E = 8$°C	46.67	67.73	105.19	1.468	27.663	35.067	50	69	106	1.469	27.50	35.48
$T_C = T_A = 35$°C, $T_E = 8$°C	53.22	72.25	110.51	1.423	25.674	39.43	50	71	109	1.411	25.76	39.18
$T_C = T_A = 38$°C, $T_E = 8$°C	56.27	76.94	116.50	1.316	22.677	47.171	50	75	116	1.273	22.02	49.08
$T_C = T_A = 35$°C, $T_E = 5$°C	56.36	73.52	112.91	1.300	23.021	46.134	50	72	113	1.270	22.47	47.70

6.8 Summary

A GA based optimization tool was developed to couple with the double effect series and parallel flow type VARS configurations, to find the optimal combinations of HPG and LPG temperatures for the double effect series and adittionally, the optimal *D* for the double effect parallell configuration. The optimization was done for both H_2O–LiCl and H_2O–LiBr operated double effect absorption cooling systems, to obtain the optimal operating parameters for four different test cases of fixed condenser (also equal absorber) and evaporator temperatures. The conclusions made from this optimization study are listed below.

- The optimal combinations of HPG and LPG temperatures obtained during four different test cases were found to be low for the H_2O–LiCl operated double effect series and parallel systems compared to those of H_2O–LiBr. For both the solution pairs, the optimal HPG and LPG temperatures were found to increase proptionately with increase in condenser (also absorber) temperature in the double effect series and parallel systems. The optimal HPG and LPG temperatures however decreased with increase in evaporator temperature at fixed condenser and absorber temperatures.
- The optimal distribution ratios obtained during various test cases with respect to the double effect parallel system, were found to be slightly higher in the range from 46.67–56.36% for H_2O–LiCl than those of H_2O–LiBr (range: 40.79–47.32). Further for the H_2O–LiCl operated double effect parallel system, the optimal distribution ratio showed a proportional increase with increase in condenser (also absorber) temperature. With H_2O–LiBr, however, no such specific trend was observed.
- For all cases of fixed condenser, absorber and evaporator temperatures, the optimum COPs of the double effect series and parallel systems were found to be slightly lower for H_2O–LiCl than those of H_2O–LiBr. However, for the H_2O–LiCl operated systems, the exergy efficiencies were higher at the optimized operating conditions.
- Most importantly, at the optimized conditions, for a given case of fixed condenser (also equal absorber) and evaporator temperatures, the total VARS irreversibility was significantly less in the H_2O–LiCl operated double effect

series and parallel systems compared to that of the H_2O–LiBr.

- With an exception in Case 1, at optimal condition of minimum irreversibility (also maximum exergy efficiency), the performance of the double effect H_2O–LiCl parallel configuration was found superior to H_2O–LiBr, not only in terms of higher exergy efficiency and lower total irreversibility but also in terms of slightly higher COP.
- The GA based optimization program which was developed in this Chapter can be used to estimate the optimal HPG and LPG temperatures of the double effect series and additionally the distribution ratio of the parallel system, corresponding to any fixed set of condenser, absorber and evaporator temperatures.
- Thermo economic/Exergoeconomic optimization, involving total cost rate and the cost rate of exergy destruction as objective functions, may be another possible future work in this area to find out more details regarding optimal performance of the double effect absorption cooling systems.

Bibliography

[1] Patek, J. and Klomfar, J. Thermodynamic properties of the LiCl–H_2O system at vapour–liquid equilibrium from 273 K to 400 K. *International Journal of Refrigeration,* 31:287–303, 2008.

[2] Gomri, R. and Hakimi, R. Second law analysis of double effect vapour absorption cooler system. *Energy Conversion and Management,* 49: 3343–3348, 2008.

[3] Farshi, L. G., Mahmoudi, S. M. S., Rosen, M. A., and Yari, M. A. Comparative study of the performance characteristics of double-effect absorption refrigeration systems. *International Journal of Energy Research*, 36:182–192, 2012.

[4] Patek, J. and Klomfar, J. A computationally effective formulation of thermodynamic properties of LiBr–H_2O solutions from 273 to 500 K over full composition range. *International Journal of Refrigeration,* 29: 566–578, 2006.

[5] Wagner, W., Cooper, J. R., Dittmann, A., Kijima, J., Kretzschmar, H. J., Kruse, A., et al. The IAPWS Industrial Formulation 1997 for the thermodynamic properties of water and steam. *Journal of Engineering, Gas Turbine Power,* 122:150–81, 2000.

[6] Goldberg, D. E. Genetic Algorithms in Search Optimization and Machine Learning. MA Reading: Addison-Wesley, 1989.

[7] Mitchell, M. An Introduction to Genetic Algorithms. MIT Press, Cambridge, London, England, 1989.

[8] Won, S. H. and Lee, W. Y. Thermodynamic Design Data for Double–Effect Absorption Heat Pump Systems Using Water-Lithium Chloride Cooling. *Heat Recovery Systems and CHP,* 11: 41−48, 1991.

[9] Bellos, E., Tzivanidis, C., Pavlovic, S., and Stefanovic, V. Thermodynamic investigation of LiCl–H_2O working pair in a double effect absorption chiller driven by parabolic trough collectors. *Thermal Science and Engineering Progress,* 3:75–87, 2017.

[10] She, X., Yin, Y., Xu, M., and Zhang, X. A novel low-grade heat-driven absorption refrigeration system with LiCl–H_2O and LiBr–H_2O working pairs. *International Journal of Refrigeration,* 58:219–34, 2015.

[11] Deka, A. and Datta, D. B-spline curve based optimum profile of annular fins using multiobjective genetic algorithm. *Journal of Thermal Stresses*, 40 (6):733–746, 2018.